Influence of dielectric layer on negative refractive index and transmission of metal-dielectric-metal sandwiched metamaterials

Min Zhong (钟 敏)[1,2]

[1]*Department of Physics, Nanjing Normal University, Nanjing 210023, China*

[2]*Hezhou College, Hezhou 542899, China*

Corresponding author: zhongmin2012hy@163.com

Received October 21, 2013; accepted March 5, 2014; posted online April 4, 2014

Transmission and negative refractive index (NRI) of metal-dielectric-metal (MDM) metamaterials perforated with different thickness of dielectric layer are studied. It can be found that transmission peaks of rectangular hole are sensitive to the thickness of the dielectric layer. NRI and the bandwidth of NRI are increased with the increasing of the thickness of dielectric layer. NRI of rectangular hole with the thickness of dielectric layer almost follows a linear law when the thickness of dielectric layer in 2–5 μm. A high NRI of metamateriral can be obtained by adjusting the thickness of the dielectric layer of the rectangular hole on MDM metamateriral arrays.

OCIS codes: 160.3918, 160.4236, 260.1180, 260.3910, 160.5298.

doi: 10.3788/COL201412.041601.

Metamaterials have attracted much attention recently due to their unique properties, such as negative refractive index(NRI) and extraordinary transmission (EOT)[1−3]. One kind of metamaterials, the metal-dielectric-metal (MDM) sandwich metamaterials is one of the most typical design, which has attracted lots of research interests[4−7]. Both EOT and NRI phenomena have been observed in the MDM sandwich metamaterials, and these phenomena are widely studied over the past decade in literature[8−11]. The shape and periodicity of metamaterials profoundly affects the extraordinary transmission phenomenon. The central wavelength of the transmitted peak intensity can be substantially affected and the normalized transmission can also be enhanced through changing the shape of the holes[12]. In 2005, Garcı′a-Vidal *et al*[13] suggest that the transmittance can be greatly boosts through filling a dielectric in the hole. However, these studies didn't consider the influence of the thickness of dielectric layer on properties of MDM sandwiched metamaterials. In order to study the influence of the thickness of dielectric layer on properties of transmission and NRI, transmission spectra and negative refractive spectra are studied with different thickness of dielectric layer.

One unit cell of the MDM structure is shown in Fig. 1(a). Dimensions of MDM in Fig. 1(a): a rectangular hole of sides $a = 6$ μm and $b = 2$ μm perforated on a MDM metamaterials. The thicknesses of the silver film and the SU-8 layer are $s = 0.05$ μm and $h = 2$ μm, respectively. The lattice constant in the x-y plane is $P = 12$ μm. Our sample contains three films: two silver films are separated by one SU-8 membrane which perforated with a square array of rectangular holes. The sample is fabricated as follow: firstly, the optical lithography is used to fabricate the freestanding SU-8 layer with rectangular hole[14]. Secondly, the silver layer is deposited on the surface of the SU-8 layer by thermal evaporation. Finally, a scanning electron microscope (SEM) (JSM-5610LV, JEOL, Japan) is employed to get the image of sample, which is shown in Fig. 1(b). Apertures of the sample are well defined and the surface of the sample is smooth across a 5×5 (mm) area. The process working pressure and deposition time are 55e-10 (atm) and almost two hours, respectively. And in this letter, all of numerical calculation results are based on the SEM image in Fig. 1(b).

An Optics Fourier transform infrared spectrometer (Equinox, Bruker, Germany) is used to measure the transmittance spectra at normal incidence. The measurement result is shown in Fig. 1(c). And the polarization is the same as the Fig. 1(a). It can be found that there are three transmittance bands in 10–25 THz, and frequency centers of these transmittance bands are located at around 13.05, 19.4 and 23.2 THz, respectively. The commercial software Ansoft HFSS12 is used to do the simulation. In simulation, the polarized wave propagates along the z axis (**k**), the electric field is in the y axis (**E**), and the magnetic field is in the x axis (**H**), respectively. The dielectric constant of SU-8 is assumed

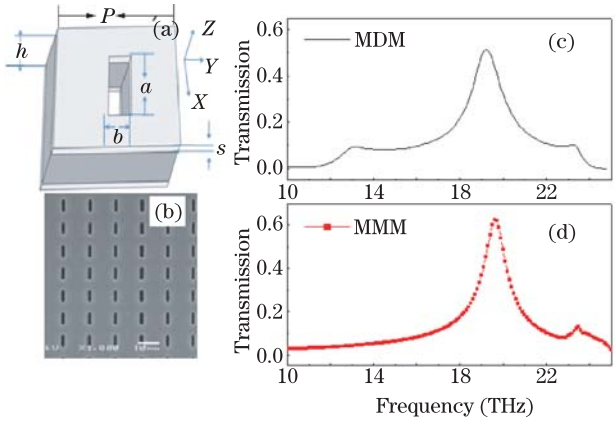

Fig. 1. (a) Scheme of one unit cell of the MDM structure. (b) SEM image of the sample. (c) Transmittance spectra of the MDM structure. (d) Simulated transmittance spectra of the metal- metal -metal (MMM) structure.

to be $2.56 + 0.035i$[15]. The silver layer uses the Drude model:

$$\varepsilon(\omega) = 1 - \frac{\omega_{\mathrm{p}}^2}{\omega^2 - \mathrm{i}\omega\gamma_{\mathrm{D}}}. \quad (1)$$

Here, the collision frequency is $\gamma_{\mathrm{D}} = 9\times10^{13}\ \mathrm{s}^{-1}$, and the plasma frequency is $\omega_{\mathrm{p}} = 1.37\times10^{16}\ \mathrm{s}^{-1}$[16]. Two ideal magnetic conductor planes are utilized on the boundary normal to the x axis and two ideal electric conductor planes on the boundary normal to the y axis in the simulation[17]. The whole model is tested in air and light incident from air to our structure propagates along the z axis. One can obtain the S parameters, transmittance and negative refractive by using the unit cell[11]. To find the potential physics behind the low frequency transmittance band, the SU-8 layer of the MDM structure in Fig. 1(a) is changed to silver layer, to get a MMM structure. And the simulated transmission spectrum of the MMM structure is also shown in Fig. 1(d). As shown in Fig. 1(d) that the low frequency transmission band disappears but two higher frequency bands are still remained in the MMM structure. At the same time, the electric field distribution at $f = 13.05$ THz between silver layer and SU-8 layer (MDM structure), silver layer and silver layer(MMM structure) are shown in Fig. 2.

It is obviously that the electric field amplitude concentrates inside the rectangular hole and in the interlayer in MDM structure. But the electric field distribution disappears when in MMM structure. These results in Fig. 2 indicates that the low frequency band in Fig. 1(c) is from the internal surface plasmon polaritons (SPPs). Moreover, the S parameters retrieval methods is used to acquire the refractive index of MDM structure and MMM structurealong the incident direction[16,17], which are shown in Fig. 3. There is a negative refractive index (NRI) band around the low-frequency transmittance band, as shown in Fig. 3(a). But the NRI band disappears when the electric field distribution disappears in MMM structure, as shown in Fig. 3(b).

In the latter simulation, the dielectric layer thickness will be changed from 2 to 3, 4, and 5 μm to investigate the influence. The simulated transmittance spectra with different thickness are shown in Fig. 4. Maximum transmission peaks are 0.51 (2 μm), 0.47 (3 μm), 0.43 (4 μm), 0.22 (5 μm), respectively. All of transmittance peaks are reduced with the thickness of the dielectric layer increasing. It is due to the dielectric loss of SU-8 is increased with the thickness of the dielectric layer increasing. It is obviously that high-frequency transmittance peaks are red-shifted, but low-frequency transmittance peaks are blue-shifted. These results indicate that transmittance peaks of MDM metamaterial with rectangular holes array are sensitive to the thickness of dielectric layer.

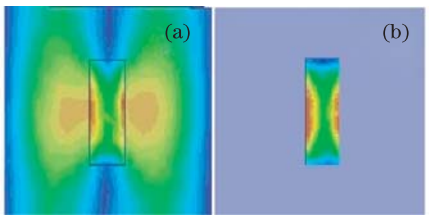

Fig. 2. Electric field distribution at $f = 13.05$ THz: (a) MDM structure; (b) MMM structure.

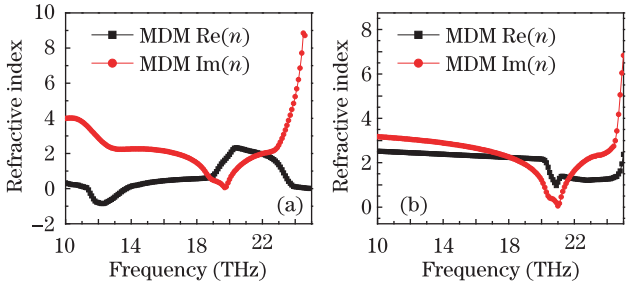

Fig. 3. (a) Refractive index of the MDM structure; (b) refractive index of the MMM structure.

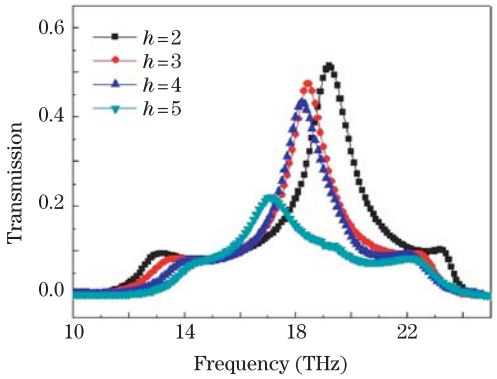

Fig. 4. Transmittance spectra with different thicknesses of dielectric layer (2, 3, 4, and 5 μm).

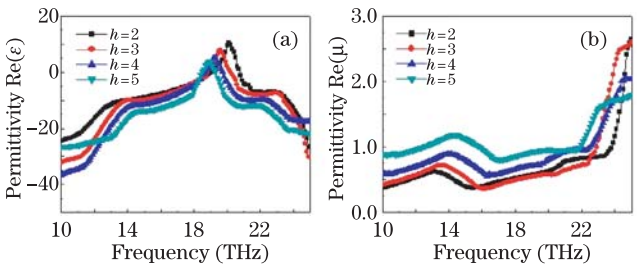

Fig. 5. Permittivity and permeability spectra with different thicknesses of dielectric layer ($h = 2$, 3, 4, and 5 μm).

In 2008, Mary *et al.*[18] suggested that the resonance magnetic response can lead to negative refractive index. In order to have a deeper insight into the electromagetic response of the low-frequency transmittance band, especially the NRI, the S parameters retrieval methods is used to acquire the refractive index, permeability and permittivity along the incident direction[16–19]. The retrieved effective permittivity ε and permeability μ are shown in Fig. 5. And the refractive index with different thickness of dielectric layer is shown in Fig. 6. On one hand, it is obviously that the real part of the effective permittivity ε exhibits a Drude-like electric response, as shown in Fig. 5(a). This leads to the transmittance exhibits a significant increased from frequency 12 to 15 THz, as shown in Fig. 4. On the other hand, the real part of the effective permeability μ exhibits a Lorentz-like magnetic response, as shown in Fig. 5(b). However, in the NRI band, the $\mathrm{Re}(\varepsilon) < 0$, but the $\mathrm{Re}(\mu) > 0$, a single negative index material can be obtained[11,20].

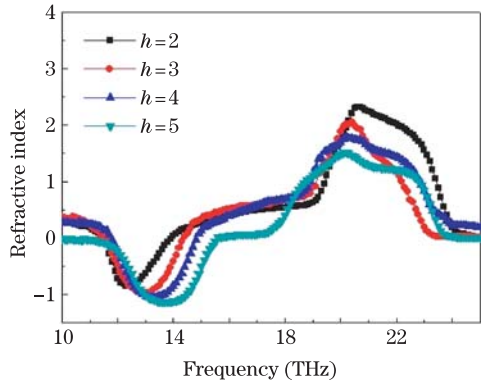

Fig. 6. Refractive index spectra with different thicknesses of dielectric layer (h = 2, 3, 4, and 5 μm).

Table 1. NRI and NRI Bandwidth as a Function of the Thickness of Dielectric Layer

Thickness (μm)	h=2	h=3	h=4	h=5
NRI	–0.85	–0.96	–1.05	–1.12
Bandwidth (Thz)	2.3	2.7	3	4.7

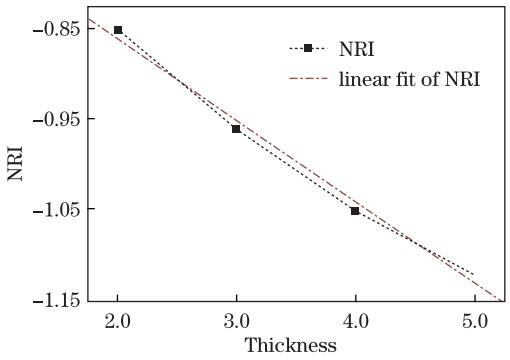

Fig. 7. (Color online) NRI with different thicknesses of dielectric layer. The red line is the numerical fitting result.

It can be found that NRI appears from 12 to 15.4 THz which is almost consists with the low-frequency transmittance peak. The central frequency of NRI band is blue-shifted which is consisted with the low-frequency transmittance band. The NRI and the NRI bandwidth are increased with the thickness of dielectric layer increasing, as shown in Table 1.

At the same time, in order to find out the relationship between the thickness of dielectric layer and NRI, the Origin8.0 software is used to numerical fitting to get a linear equation:

$$y = a + b \cdot x, \tag{2}$$

where x indicates thickness and y indicates NRI. The intercept is $a = -0.68$ and the slop is $b = -0.09$. The result of fitting is the red line, as shown in Fig. 7. It can be found that NRI of MDM metamaterials with rectangular holes array with different thickness of dielectric layer almost follows a linear law in 2–5 μm.

In conclusion, the influence of thickness of dielectric layer on transmission and NRI of MDM sandwiched metamaterial has been studied. In the middle-infrared region, transmittance peaks exhibit different performance with the thickness of dielectric layer increasing: (1) the maximum transmittance peak is red-shifted; (2) the low-frequency transmission peak is blue-shifted. NRI and the bandwidth are increased with the thickness of dielectric layer increased in 2–5 μm. NRI of rectangular hole with the thickness of dielectric layer almost follows a linear law when the thickness of dielectric layer in 2–5 μm. One can obtain a high NRI metamateriral by increasing the thickness of dielectric layer on MDM metamateriral arrays.

This work was supported by the National Natural Science Foundation of China (No. 60778041), the Natural Science Foundation of the Jiangsu Higher Education Institutions of China (No. 07KJA51001), and the Graduate Research and Innovation Program of Ordinary University of Jiangsu Province (Nos. 2011ZRKY06 and 2012ZRKY04).

References

1. L. Wang, Z. S. Wang, T. Sang, F. L. Wang, Y. G. Wu, and L. Y. Chen, Chin. Opt. Lett. **6,** 030198 (2008).
2. H. Yin, Y. Liu, Z. Yu, Q. Shi, H. Gong, X. Wu, and X. Song, Chin. Opt. Lett. **11,** 101901 (2013).
3. C. Helgert, C. Menzel, C. Rockstuhl, E. Pshenay-Severin, E. B. Kley, A. Chipouline, A. Tunnermann, F. Lederer, and T. Pertsch, Opt. Lett. **34,** 704 (2009).
4. C. Imhof and R. Zengerle, Appl. Phys. A **94,** 45 (2009).
5. C. Helgert, C. Menzel, C. Rockstuhl, E. Pshenay-Severin, E. B. Kley, A. Chipouline, A. Tunnermann, F. Lederer, and T. Pertsch, Opt. Lett. **34,** 704 (2009).
6. P. Ding, E. J. Liang, W. Q. Hu, Q. Zhou, L. Zhang, Y. X. Yuan, and Q. Z. Xue, Opt. Express **17,** 2198 (2009).
7. Z. Ku, J. Zhang, and S. R. J. Brueck, Opt. Express **17,** 6782 (2009).
8. J. B. Pendry, Phys. Rev. Lett. **85,** 3966 (2000).
9. F. Wang, H. Liu, T. Li, Z. Dong, S. Zhu, and X. Zhang, Phys. Rev. E **75,** 016604 (2007).
10. R. Ortuno, C. Garcia-Meca, F. J. Rodriguez-Fortuno, J. Marti, and A. Martinez, Phys. Rev. B **79,** 075425 (2009).
11. S. Zhang, W. Fan, N. C. Panoiu, K. J. Malloy, R. M. Osgood, and S. R. J. Brueck, Phys. Rev. Lett. **95,** 137404 (2005).
12. K. J. Klein Koerkamp, S. Enoch, F. B. Segerink, N. F. van Hulst, and L. Kuipers, Phys. Rev. Lett. **92**, 183901 (2004).
13. F. J. García-Vidal, L. Martín-Moreno, E. Moreno, L. K. S. Kumar, and R. Gordon, Phys. Rev. B **74,** 153411 (2006).
14. Y. Ye, D. Y. Jeong, and Q. M. Zhang, Appl. Phys. Lett. **85,** 654 (2004).
15. Y. Hua and Z. Li, J. Appl. Phys. **105,** 013104 (2009).
16. D. R. Smith, D. C. Vier, T. Konschny, and C. M. Soukoulis, Phys. Rev. E **71,** 036617 (2005).
17. D. R. Smith, S. Schultz, P. Markos, and C. M. Soukoulis, Phys. Rev. B **65,** 195104 (2002).
18. A. Mary, S. G. Rodrigo, F. J. Garcia-Vidal, and L. Martin-Moreno, Phys. Rev. Lett. **101,** 103902 (2008).
19. R. A. Depine and A. Lakhtakia, Microwave Opt. Technol. Lett. **41,** 315 (2004).
20. U. K. Chettiar, A. V. Kildishev, H. K. Yuan, W. S. Cai, S. M. Xiao, V. P. Drachev, and V. M. Shalaev, Opt. Lett. **32,** 1671 (2007).